Microevolution of Bank Voles (*Myodes glareolus*) at Neutral and Immune Related Genes During Multiannual Dynamic Cycles: Consequences for Puumala hantavirus Epidemiology

Adelaïde Dubois[1,2*], Maxime Galan[1], Jean-François Cosson[1,3], Bertrand Gauffre[4], Heikki Henttonen[5], Jukka Niemimaa[5], Maria Razzauti[1], Liina Voutilainen[5,6], Renaud Vitalis[1], Emmanuel Guivier[7], Nathalie Charbonnel[1]

[1] INRA, UMR1062 CBGP, 755 avenue Campus Agropolis, 34980 Montferrier-sur-Lez, France

[2] Anses, Unité de Virologie, 31 avenue Tony Garnier, 69364 Lyon, France

[3] INRA-ANSES-ENVA, UMR 0956 BIPAR, Maisons-Alfort, France.

[4] INRA, USC1339 (CEBC-CNRS), Villiers en Bois F-79360, France

[5] Natural Resources Institute Finland, FI-013012 Vantaa, Finland

[6] Department of Virology, University of Helsinki, FI-00014 University of Helsinki, Finland

[7] Biogeosciences, CNRS UMR 6282, Université de Bourgogne, Franche-Comté, 21000 Dijon, France

* Email: adelaide.dubois@supagro.inra.fr

Short title: Microevolution of Bank Vole Metapopulation

Keywords: population genetics;immune related gene;adaptation; selection ; host pathogen interaction ; microevolution ; dynamic fluctuations ; Puumala ; virus ; rodent ; Myodes glareolus ; bank vole ; epidemiology

Abstract

Understanding how host dynamics, including spatiotemporal variations of population size and dispersal, may affect the epidemiology of infectious diseases is an active research area. Population dynamics drive neutral and adaptive micro-evolutionary processes that in turn, influence pathogens persistence, their distribution and evolution. This study focuses on a bank vole (*Myodes glareolus*) metapopulation surveyed in Finland between 2005 and 2009. Bank vole is the reservoir of Puumala hantavirus (PUUV), the agent of nephropathia epidemica (NE, a mild form of hemorrhagic fever with renal symptom) in humans. *M glareolus* populations experience multiannual density fluctuations that have previously been related to the level of genetic diversity maintained in bank voles, variations in PUUV prevalence and NE occurence in humans. Here, we examine the potential impacts of vole metapopulation genetics on PUUV epidemiology. Using microsatellite markers, we evaluate the impact of density cycles on genetic drift and host gene flow. We show that genetic drift slightly and transiently affects neutral and adaptive genetic variability within the metapopulation. Gene flow seemed to counterbalance its effects during the multiannual density fluctuations. The low abundance phase may therefore be too short to impact genetic variation in the host, and consequently viral genetic diversity. We did not detect any environmental heterogeneity affecting vole gene flow, which might explain the absence of spatial structure previously detected in PUUV in this area. We found evidence for the role of vole dispersal on PUUV circulation through sex-specific and density-dependent movements. We further analyzed how multiannual dynamic cycles affected selection acting on immune related genes involved in susceptibility to PUUV. We detected associations between *Mhc-Drb* haplotypes and PUUV serology, and density related patterns of departures from neutrality on *Tnf* promoter, *Tlr-4* and *Mx2* genes. They could reflect signatures of positive and balancing selection acting on these genes, which might influence PUUV microevolution. Altogether, this study provides an original framework for population genetics research developed in epidemiological contexts.

Introduction

Molecular epidemiology has largely focused on the parasite side, contributing to a better understanding of transmission patterns and factors influencing disease spread. Host population genetics can also be of great importance to analyze pathogen persistence, spread and evolution, although it has been overlooked (1). Indirect approaches based on population genetics can highlight local variations in host genetic diversity that are due to natural fluctuations in host population size, a central parameter in epidemiology. Besides, many parasites lack free-living stages or have limited dispersal capacities and are therefore highly dependent of their hosts to disperse (2). When disease transmission is specifically associated with a given host species, host population genetics can reveal environmental heterogeneity that may affect the propagation of diseases by reducing both movements of infected hosts and contacts between infected and non-infected ones (3). In this context, Cullingham et al. (4) showed that rivers could act as barriers to raccoon dispersal in Quebec, therefore limiting the propagation of raccoon rabies. Hence, by identifying landscape characteristics affecting wildlife dispersal, such studies could help predicting the spread of diseases and developing proactive disease management. The analysis of adaptive genetic variation, especially that linked to host–pathogen interactions, should also improve our knowledge of disease epidemiology (see for a review 7). Immune related gene polymorphism may be affected by genetic drift (e.g 8–10), but several studies have revealed that selection could rapidly buffer the loss of adaptive diversity in bottlenecked populations (9,10).

The development of host population genetics in epidemiological contexts might be highly relevant when populations exhibit multiannual density cycles. Such dynamics can lead to variations of effective population size (11) that may significantly affect genetic diversity and population genetic structure. Drastic reductions in population size can cause a rapid decrease of allelic diversity and a gradual erosion of heterozygosity, with negative consequences on adaptive potential (12–14). However a high level of genetic diversity may sometimes persist in these populations, both at neutral and immune related genes (10,15–19). Density cycles can also impact dispersal rates, and consequently the distribution of genetic variability within and among populations. Several studies showed that cyclic populations of the fossorial water vole were weakly differentiated during the

increasing phase of abundance, suggesting high migration rate among demes, but highly differentiated during the low phase of abundance, as a result of local genetic drift and low dispersal rates (16,20). Such cyclic dynamics could therefore have severe consequences on disease epidemiology, both ecologically and evolutionarily. Up to now, most of the studies dedicated to the genetics of these cyclic populations have been realized in the context of agricultural damages. The links with epidemiological risks still remain to be explored.

In this study, we examined this triptych relationship between host density cycles, population genetics and epidemiology of a viral infection in the bank vole (*Myodes glareolus*) and Puumala virus (PUUV, family of *Bunyaviridae*) as model species. In boreal Fennoscandia, bank vole populations undergo three to five year density cycles with high amplitude (21,22). The bank vole is the reservoir of PUUV, the etiologic agent of nephropathia epidemica (NE) (23). Among voles, the virus is transmitted horizontally through contacts between individuals (*i.e*. bites) or via infectious aerosolized urine and feces (24). The spread of PUUV is therefore closely linked to its host dispersal. PUUV infection in bank voles is chronic and asymptomatic (24–26) although maturation, winter survival and female breeding of infected individuals may be affected (27–29). The epidemiology of PUUV in rodent populations has been well documented (30). Only two studies have yet examined the connection between bank vole population and PUUV dynamics. Guivier et al. (31) developed a landscape genetics approach to analyze the influence of bank vole population dynamics on PUUV spatial distribution in contrasted landscape structure. They considered genetic diversity as a proxy for estimating vole population size, isolation and migration, and found that it was highly positively correlated with PUUV prevalence and with the abundance of forest habitats at a local scale. This suggested that the persistence of PUUV was enhanced in lowly fragmented forests, where vole metapopulations are highly connective and experience low extinction rates. Besides, Weber de Melo et al. (32) made a comparative analysis of the spatio-temporal population genetic structure of bank voles and PUUV at a smaller spatial scale. They aimed at testing the influence of vole neutral microevolutionary processes on PUUV phylodynamics. They found incongruent patterns between host and PUUV population genetic structure that were likely to arise due to the high evolutionary rate of this virus.

What is still missing to better understand the links between PUUV epidemiology and bank vole metapopulation dynamics is the characterization of the microevolutionary processes at play in the genes known to influence rodent susceptibility to hantaviruses (review in 32). To bridge this gap, we analyzed the genetics of bank voles at presumably neutral and immune related genes in a metapopulation monitored during a whole demographic cycle in an endemic area of Finland. The microevolution of PUUV was recently examined by Razzauti et al. (34) in a large geographic area including this metapopulation. They showed the weak impact of host population cycles on the levels of viral genetic diversity, the high local turn-over of PUUV variants (RNA virus) and the absence of spatial structure in the viral population. We first examined the consequences of drastic density variations on the dynamics of neutral and adaptive genetic diversity in *M. glareolus* populations, both at the metapopulation scale and at a finer scale. Second, we performed population genetics analyses to search for spatial barriers, as lake or rivers, that could affect gene flow among vole populations and therefore the circulation of PUUV. We also tested whether PUUV transmission was likely to result from vole dispersal or contacts between relatives (35). Third, we sought to disentangle the effects of drift, migration and selection acting on vole immune related genes. To this aim, we compared the genetic structure observed at these genes with the one detected using presumably neutral microsatellite loci. Departures from neutral expectations could be mediated by selection. We also looked for associations between immune related gene polymorphism and susceptibility to PUUV. These latter analyses enabled to investigate the possibility that selective forces may shape bank vole / PUUV interactions despite the pronounced multiannual density cycles.

Materials and Methods

Ethic statement

All handling procedures of wild live bank voles followed the Finnish Act on the Use of Animals for Experimental Purposes (62/2006) and took place with permission from the Finnish Animal Experiment Board (license numbers HY 45-02, HY 122-03, and HY 54-05). The ethics committee

approved this study. All efforts were made to minimize animal suffering. The species captured for this study, *Myodes glareolus*, neither is protected nor included in the Red List of Finnish Species. The animal trapping took place with permission from the landowners

Rodent sampling and PUUV detection

Rodents were trapped within an area of about 25 km² of typical spruce-dominated taiga forest at Konnevesi, Central Finland (62° 34' N, 26° 24' E), where PUUV is highly endemic (27,30,36). Trappings for bank vole genetic materials were carried out between 2005 and 2009 to include a whole density cycle (peak year 2005, decline 2006, increase 2007, peak 2008, decline 2009, see (18,24,34), Fig. 1). Too few individuals could be sampled in crash year 2006 so that it was not included in the study. Trapping sessions included here were conducted in the beginning and middle period of the breeding season (May, July in 2005, 2008) or in October (2007, 2009) to gather enough individuals during these low abundance years. Nine sites situated at least 750m apart from each other within 25 km^2 were sampled (Fig. 1). Briefly, a grid of 3 x 3 Ugglan Special live traps (Grahnab AB, Sweden) with 15 m intervals and baited with oat seeds and potato was set in each site. Traps were checked once a day during three days, and captured bank voles were brought into the laboratory, bled through retro-orbital sinus, sacrificed, weighed, measured and sexed (for details, see Voutilainen et al. (30). Tissue samples (toe or tip of the tail) were collected and stored in 95% ethanol for further genetic analyses. The heart of each animal was collected, diluted into 200 µL phosphate-buffered saline and frozen for latter PUUV antibody analysis. Detection of PUUV was done as described in Kallio-Kokko et al. (37). Serological and virological data have previously been described in Voutilainen et al. (24,30,38) and Razzauti et al. (39). Because PUUV infection in bank voles is chronic, the presence of PUUV antibodies was taken as an indicator of infection (26), except for juvenile voles trapped in July because of the possible presence of maternal antibodies (40,41). In this case, seropositive bank voles with low body mass (<17.5g, see 30) were considered to be juveniles carrying maternal antibodies but not PUUV infected (21 bank voles were concerned and were not considered in the analyses including seroprevalence). Sampling size and seroprevalence levels are described in details in Table S1.

Fig 1. Map of the study area and long term fluctuations of bank voles in Konnevesi.

A) The nine trapping sites included in this study are indicated by a red square. These sites were situated at least 750 m apart. The location of Konnevesi within Finland is shown on the right box. B) Total bank vole abundance and number of infected voles trapped per 100 trap nights in the nine Konnevesi sites considered in this study between 2005 and 2009 (from 29). White circles represent sampling dates.

DNA extraction and loci amplification

Microsatellite analyses – We analyzed 402 bank voles. Genomic DNA was extracted using the DNeasy 96 Tissue kit (Qiagen) according to manufacturer's recommendations. A final elution was done in 400µl of AE buffer (Qiagen). Samples were first genotyped at 19 unliked microsatellites loci previously published by Rikalainen et al. (42) using primers and cycling conditions described in Guivier et al. (31). Genotyping was carried out using an ABI3130 automated DNA sequencer (Applied Biosystems). Alleles were scored using GENEMAPPER software (Applied Biosystems). Two loci were excluded from the genetic analyses: Cg6G11 because of the poor quality profiles obtained and Cg5F11 because it was duplicated in these populations.

Candidate gene analyses - The polymorphism of candidate genes that are relevant with regard to PUUV infections was further analyzed. These candidate genes, namely *Mhc-Drb, Tnf-α* promoter, *Mx2, Tlr4* and *Tlr7,* were selected based on the literature of rodent or human/hantavirus interactions (33,43). The second exon of the *Mhc-Drb* class II is a highly polymorphic gene of the major histocompatibility complex. It encodes for proteins responsible for pathogen recognition (44). *Tlr4* and *Tlr7* genes encode for Toll-like receptors which play an important role in activating the innate immune system (45). TLR4 is a universal receptor able to detect different ligands as LPS of Gram-negative bacteria and also some viral proteins (46) including hantaviral proteins (47). TLR7 is a receptor to virus, which is probably involved in the detection of ssRNA viruses like hantaviruses (48). As both *Mhc* and *Tlr* genes encode for receptors, their polymorphism is likely to be linked to the efficiency of antigen recognition. *Tnf* (Tumour Necrosis Factor alpha) gene

encodes for a cytokine involved in the pro-inflammatory response (49,50). Polymorphism within the *Tnf* promoter seems to be, at least partly, implicated in the regulation of *Tnf* transcription and consequently in the magnitude of the secretory response of this cytokine (51,52). Mx proteins are interferon-induced members of the superfamily of large GTPases. They mediate innate, antiviral resistance in rodents, as well as in other vertebrates and humans (53,54). Most Mx GTPases inhibit a wide range of RNA viruses, including members of the *Bunyaviridae* at an early stage in their life cycle. Thus, the efficiency of antiviral resistance seems to be mediated by *Mx* genes polymorphism.

The second exon of the *Mhc-Drb* class II was genotyped using a 454 Genome Sequencer FLX (Roche) with the procedure detailed in Galan et al. (55). The locus was amplified using a modified version of the primers JS1 (5'- GCCTCCCTCGCGCCATCAG -3') and JS2 (5'- GCCTTGCCAGCCCGCTCAG -3') initially designed for a lemur (56). Individual-specific MIDs (Multiplex Identifiers) and 454 adaptors required for the emPCR and the 454 GS-FLX sequencing were also added (for more details concerning laboratory procedures, see 57,59). The SESAME barcode software (SEquence Sorter & AMplicon Explorer, 60) was used to sort sequences, identify and discard artefactual variants, and generate the allele sequences and individual genotypes. The *Drb*-exon2 sequences were aligned in the BioEdit sequence alignment editor (59) using CLUSTAL X Multiple Alignment v7.0.9.0 (60). Nomenclature of the bank vole sequences follows Klein et al. (61). The sequences are available in GenBank under accession numbers HM347503–HM347507 and HM107849–HM107870. Human *Homo sapiens* (GenBank accession numbers 91M17236 and AM109973), sheep *Ovis aries* (M33304, AY230000) and pig *Sus scrofa* (M29938, NM_001113695) sequences were used as outgroups in phylogenetic analyses. MEGA4 software (62) was employed to construct a phylogenetic tree of the *Drb*-exon2 gene using the neighbour-joining algorithm and Kimura two-parameter distance model. A bootstrap analysis (1000 replicates) was performed to determine the reliability of the branching. We confirmed that *Drb*-exon2 was at least duplicated in *M. glareolus* (63). Although phylogenetic reconstructions did not enable us to assign all alleles to one or another copy of the gene, we identified unambiguously different alleles as belonging to the

monophyletic allele cluster I defined by Axtner et al. (63). All other alleles were not considered in the analyses.

Polymorphisms of *Tnf* gene promoter, *Mx2* exons 13 and 14, *Tlr4* cDNA, and *Tlr7* gene were previously investigated by the sequencing of bank voles sample from several European countries (unpublished data, see technical details in S1 protocol). At the European scale, we identified seven Single Nucleotide Polymorphisms (SNPs) in *Tnf* gene promoter, four SNPs in *Mx2* exons 13 and 14, ten SNPs in *Tlr4* gene, and one SNP in *Tlr7* gene. Based on this previous pilot study, we further selected eight polymorphic SNPs found in bank voles from Fennoscandia and the 402 individuals from Konnevesi were genotyped using the KASPar allelic-specific fluorescent genotyping system provided by KBiosciences (Hoddesdon, UK).

Statistical analyses

Within site and within metapopulation genetic diversity – As the number of voles trapped per site could be low, we pooled samples from May and July for each site. Moreover, because 2009 was a low-density year, we pooled all samples from all sites between May and October for this year. Further analyses were realized at two different spatial scales for each year: for each site and over the whole metapopulation. We tested the conformity to Hardy-Weinberg equilibrium (HWE) for each locus and we analyzed linkage disequilibrium (LD) for each pair of loci using GENEPOP v4.2 (64). Corrections for multiple tests were performed using the false discovery rate (FDR) approach as described in Benjamini & Hochberg (65). For all microsatellites and for each immune gene (*Mhc-Drb, Tnf, Mx2*, *Tlr4* and *Tlr7*), we estimated N_a, the estimate of allelic richness corrected for minimum sample size (8 in our case) (66,67), the observed (H_o) and Nei's unbiased expected (H_e) heterozygosities (68) and Weir & Cockerham's inbreeding coefficient F_{IS} (69). Significance of F_{IS} (excess or deficit in heterozygotes) was assessed using 1000 permutations of alleles within each site. Similar estimates were obtained over the whole metapopulation. Calculations and tests were realized using GENETIX v4.05.2 (70), using FDR corrections. For these analyses, sites*years with less than eight individuals were not considered in order to avoid statistical biases.

To test whether these indices of within site and metapopulation genetic diversity varied throughout the vole dynamic cycles, we focused on N_a and H_e and we defined two linear mixed models, using the lme function implemented in the nlme package for R 3.1.0 (71). Model validations were realized *a posteriori* by checking plots of the residuals. The first model included independently these indices of diversity estimated for the sites sampled in 2005, 2007 and 2008 (2009 was not included as sample sizes per site were too low). Fixed effects included the variables *year*, *site*, *type of loci* (microsatellites, SNPs, *Mhc-Drb*). We also included the pairwise interactions *year*type of loci* and *year*site*. When the pairwise interactions were non-significant, they were removed from the model. The variable *loci* was included as a random effect to reflect the fact that there were initial differences in diversity between loci. The second model included the indices of diversity calculated over the whole metapopulation for each year between 2005 and 2009 as response variables. The fixed effects *year*, *type of loci,* their pairwise interaction *year*type of loci* and the random effect *loci* were also added. For both models, significance of the fixed effects was assessed with analysis-of-deviance tables (function ANOVA). Chi-square tests with Bonferroni correction were then applied to analyze the effect of significant variables using the package phia for R.

Spatial genetic structure - We first evaluated the level of genetic isolation of each site relatively to the others. Population-specific F_{ST} values and their 95% confidence interval were estimated using the software GESTE (72). We then investigated the relationships between bank vole population dynamics and PUUV epidemiology using a logistic regression performed with the glm function implemented in R. PUUV seroprevalence was the independent variable and the explanatory variables were the main principal components of the multivariate analysis (PCA) based on the genetic parameters estimated for each site and year and performed using R.

Spatial genetic structure was described using genetic differentiation between each pair of sites estimated from microsatellite data and Weir & Cockerham's pairwise F_{ST} estimates (69). Temporal differentiation was evaluated by estimating F_{ST} values between sampling dates. We used exact tests implemented in GENEPOP v4.2 (64) to test for differentiation. FDR corrections were applied as described above. We next used analyses of molecular variance (AMOVA) implemented

in ARLEQUIN v3.5.1.2 (73) to quantity the proportions of genetic variation due to differences between years and between sites, using two hierarchical models (see Table 2 for details).

Spatial genetic clustering was performed in one analysis including all years and sites to detect potential environmental factors affecting gene flow. We used the Bayesian clustering method implemented in STRUCTURE (74), using the admixture model with correlated frequencies. We performed 20 independent runs for $K = 2$ to $K = 8$ with a Markov chain Monte Carlo (MCMC) of 10^6 iterations following a burn-in of 500,000 iterations. To determine the number of clusters (K) best fitting our multilocus genetic data set, we used the method described in Evanno et al. (75). We next used the FullSearch algorithm implemented in CLUMPP v1.1 (76) to assign individuals to clusters. Then, summary bar plots were built using DISTRUCT v1.1 (77).

We finally examined the fine-scale spatial pattern of microsatellite genetic variation using inter-individual relatedness. We estimated the *Li* coefficient (78) implemented in SPAGEDI v1.4.c (79) for each year, considering each site separately. This estimator shows a high accuracy (low bias) combined with a high precision (low variance) compared to others (80). We performed spatial autocorrelation analyses to examine how genetic similarity between pairs of individuals changed with geographical distance. This approach was applied independently for each year, and separately for males and females to emphasize potential differences in the dispersal behavior with cycle phases (18,19). We next tested whether relatedness differed among seropositive and among seronegative bank voles, by permuting individuals between these two classes. The 15 seropositive juveniles carrying maternal antibodies were removed from this analysis. Because pairwise data are non-independent, we could not directly compare relatedness estimates between these classes of individuals using standard statistical tests (81). We thus applied the procedure of Coulon et al. (82) that consists in generating 1,000 random resampling sets without replacement, such that each individual occurs only once in a given resampled set. The difference of mean relatedness D_i between the two categories tested is then calculated for each resampling set. Under the null hypothesis, D_i should follow a normal distribution centered on 0; under the alternative hypothesis, D_i should be significantly different from 0. We made no *a priori* assumption on the sign of the difference and thus computed two-sided tests. Indeed, on one hand, PUUV seropositive bank

voles could be less related than seronegative ones if PUUV transmission mainly occurs during dispersal. On the other hand, the opposite pattern is expected if PUUV transmission occurs during winter family clustering, but up to now, this pattern has only been observed in temperate zones (see 83).

Detection of signatures of selection – We first used the software package FDIST2 (84) to test for homogeneity in differentiation level, as measured by F_{ST}, across microsatellite loci that were supposed to be neutral. This method is based on the principle that genetic differentiation among populations is expected to be higher for loci under divergent selection than for the rest of the genome. The rationale here was to compute F_{ST} and the overall heterozygosity of the pooled sample at each marker, and then to compare these values to the neutral distribution of F_{ST} conditional on heterozygosity, generated by means of coalescent simulations in a symmetrical island model at migration-drift equilibrium. We used a stepwise mutation model as implemented in FDIST2. 1,000,000 simulations were performed for each analysis, assuming a 9-demes island model and $\theta = 2nN\mu = 0.1$ (where $n = 9$ is the number of demes of size N, and μ is the mutation rate). Simulations were realized for each year independently and overall years. One-tailed *p*-values were computed for each analysis (probability of getting F_{ST} values as small or smaller than the one observed). Then, in a second step, we tested the differentiation level at immune related genes (*Mhc-Drb* and SNPs), using coalescent simulations generated conditionally on the overall F_{ST} estimate calculated from the presumably neutral microsatellite markers. We used FDIST2 to analyze differentiation at *Mhc-Drb*, and a modified version of the software package DFDIST to generate bi-allelic co-dominant data (86) to analyze differentiation at SNPs. For all analyses, the maximum frequency of the most common allele allowed was set to 0.99. These analyses were realized for each year independently. Although the true demographic history of *M. glareolus* populations is likely to depart from the island model assumptions, the distribution of F_{ST} estimates so obtained should be robust to the vagaries of demographic history (85)

Association between genotypes at immune related genes and PUUV serology - Because candidate gene polymorphism was expected to be related to bank vole susceptibility to PUUV, we searched for associations between immune variations and PUUV serology which was used as a proxy of

PUUV infection status (50). This analysis was realized on the whole dataset but we excluded the 14 seropositive juveniles carrying maternal antibodies. First, we performed a Correspondence Analysis (CoA) on the genetic matrix of candidate gene polymorphism (*Mhc-Drb*: haplotypes; other candidate genes: SNPs, coded as presence/absence), using the software ADE-4 (86). Then, we realized a Discriminant Analysis (DA) using PUUV serology as a discriminant factor. The significance of the analysis was estimated by using 10,000 permutation tests. The relative risk (RR) associated with each allele of interest, as detected with DA, was estimated following Haldane (1956). The significance of the association between these alleles and vole serological status were analyzed using Fisher exact tests and Bonferroni sequential corrections.

Results

Validation of loci

Two microsatellite loci, Cg2F2 and Cg13F9, showed important deviations to HWE suggesting the presence of null alleles. They were removed from the analyses. Thus, our final dataset included 402 bank vole genotypes at 15 microsatellites loci. The 454 sequencing of *Mhc-Drb* exon 2 revealed 17 haplotypes belonging to the manophyletic allele cluster I (63). We did not observe more than two haplotypes per individual. Eighteen variable sites were detected among the 171 bp sequences, out of which eight corresponded to non-synonymous sites. Eight SNPs were genotyped over all other candidate genes: No polymorphism was found within *Tlr7;* Four SNPs appeared to be monomorphic over the five SNPs analyzed within *Tlr4* and were excluded from the data. Finally, polymorphism of a single SNP was analyzed for each of the following immune related genes: *Mx2*, *Tnf* promoter and *Tlr4*.

Within site and within metapopulation genetic diversity

A total of 43 pairs of loci exhibited significant LD over the 684 tested (6%) after FDR correction. The loci involved were not consistent among years and sites. Two out of 60 tests for deviation from

HWE were significant, and both concerned the locus Cg16H5. Table S1 gives the range of diversity estimates, across years and sites, and at the whole metapopulation scale.

Detailed results of the statistical models performed on diversity indices are presented in Table S4. Briefly, H_e and N_a estimates were always higher at microsatellite loci than at immune related genes (Within site - H_e: X^2_2 = 45.69, $p < 10^{-4}$; N_a: X^2_2 = 25.72, $p < 10^{-4}$; Within metapopulation - H_e: X^2_2= 169.20, $p < 10^{-4}$; N_a: X^2_2 = 19.48, $p = 10^{-4}$, see Fig. 2). At the local scale (within site), H_e estimates also varied among years (X^2_2 = 8.47, p = 0.015), with lower estimates observed in 2008 than in 2007, and they marginally varied among sites (X^2_4 = 9.575, p = 0.048). Other factors than 'type of loci' explained variation in N_a estimates at the metapopulation scale only. Hence N_a estimates within metapopulation varied among years (X^2_3 = 8.985, p = 0.029), with lower estimates observed in 2009 compared to 2005. We noted that the loss of alleles was of similar amplitude at microsatellites and *Mhc-Drb* (about two alleles lost over 12 between 2005 and 2009, Table 1). Interestingly, one *Mhc-Drb* variant was lost during the crash between 2005 and 2007, and was not recovered at the metapopulation scale the years after. In the opposite, 'new' *Mhc-Drb* haplotypes were detected in particular sites of the metapopulation in 2008 (e.g. Mygl-DRB*15 in site M and Mygl-DRB*08 in site F). Immune SNPs exhibited strong temporal changes compared to other loci (interaction *year * type of loci:* X^2_6 = 41.67, $p < 10^{-4}$), in particular for *Mx2*_162 and *Tlr4*_1662, where higher H_e levels were explained by the increased frequency of the less common variant (from 0.25 to 0.35 and 0.21 to 0.34 respectively).

Fig 2. Temporal variations of H_e *and* N_a estimates (mean ± SD) for the whole metapopulation, by type of locus.

Microsatellite loci are represented as triangles, *Mhc-Drb* as circle and SNPs as square. A linear mixed model was performed with the four diversity indices estimated over the whole metapopulation sampled in 2005, 2007, 2008 and 2009. Significant differences between years are indicated by asterisks (* $p < 0.05$; *** $p < 0.001$).

Spatial genetic structure

Site specific F_{ST} estimates (GESTE sotware) ranged between 0.009 and 0.063, showing various levels of genetic isolation of sites within the bank vole metapopulation (Table S1). The first axis of the PCA based on genetic parameters (PC1) explained 57.4% of the variability and revealed a strong opposition between these local F_{ST} estimates and the other genetic features describing genetic diversity, especially H_e and N_a (Fig 3A). This axis therefore illustrated the opposing impacts of genetic drift and migration on local genetic diversity. The second axis of the PCA (PC2) accounted for 36.5% of the total variability, and opposed genetic parameters reflecting the deviation from Hardy-Weinberg equilibrium within site (H_o and F_{is}). The third PCA axis (PC3) explained 5.1% of the variability and contrasted the diversity indices N_a and H_e (Fig 3B). The projection of the variable 'year' on this axis revealed that PC3 discriminated the increase phase 2007 after the decline in 2006 and peak years (2005, 2008, Fig 3C). The best and the most parsimonious model explaining PUUV prevalence using site coordinates on these three axes included PC3 only (z-value = 2.119, p = 0.034). PUUV prevalence therefore seemed mostly related to local changes in allelic richness associated with the population cycle, PUUV seroprevalence reaching higher levels during the increase year (2007).

Fig 3. Principal component analysis based on local genetic parameters estimated using microsatellites.

Correlation circles of the five genetic variables using A) PC1 and PC2, and B) PC1 and PC3. Puumala seroprevalence was included as a supplementary variable.

Spatial pairwise F_{ST} estimates ranged between 0.003 and 0.056 for microsatellites, -0.077 and 0.270 for SNPs and -0.067 and 0.109 for *Mhc-Drb*. While most of these estimates were non significant after FDR correction for microsatellites (84.5%), a few remained significant when considering respectively SNPs and *Mhc-Drb* (Table S5). At the scale of the metapopulation, temporal pairwise F_{ST} ranged between 0.003 and 0.017 at microsatellites, with high estimates corresponding to pairs of sampling date including the crash year 2009. None of these estimates were significant when considering immune related genes (Table S6).

AMOVA analyses revealed an absence of temporal genetic differentiation over the whole metapopulation whatever the loci considered, but significant variation among years within sites, with higher percentage of variation detected at *Mhc-Drb* than at microsatellites. No temporal genetic changes were detected at immune related SNPs (Table 1A, B). Over the whole survey, AMOVA revealed a weak spatial genetic structure detected using microsatellites only, and significant variation among sites within years for all loci, with higher percentage of variation detected at *Mhc-Drb* than at microsatellites or immune related SNPs (Table 1A, B).

Table 1. Analysis of molecular variance (AMOVA).

AMOVA were performed considering the five sites B, C, F, G, O sampled in 2005, 2007 and 2008 (sample size larger than 8 individuals) and the three types of loci, *i.e.* microsatellites, immune SNPs and *Mhc-Drb*. Two hierarchies were examined: A) years as groups and sites as subdivisions within years; B) sites as groups and years as subdivisions within sites.

A)

	Microsatellites				SNPs				*Mhc-Drb*			
Source of variation	*DF*	Variance components	Percentage of variation	*p*	*DF*	Variance components	Percentage of variation	*p*	*DF*	Variance components	Percentage of variation	*p*
Among years	2	-0.003	-0.04	0.731	2	-0.004	-0.743	0.865	2	-0.002	-0.394	0.761
Among sites within years	12	0.166	2.570	**$<10^{-5}$**	12	0.009	1.966	**0.036**	12	0.019	4.516	**$<10^{-5}$**
Among individuals within sites	449	6.292	97.47	**$<10^{-5}$**	443	0.482	98.78	0.064	399	0.412	95.88	**$<10^{-5}$**

B)

	Microsatellites				SNPs				*Mhc-Drb*			
Source of variation	DF	Variance components	Percentage of variation	p	DF	Variance components	Percentage of variation	p	DF	Variance components	Percentage of variation	p
Among sites	4	0.042	0.65	**0.0006**	4	-0.003	-0.553	0.677	4	0.002	0.378	0.424
Among years within sites	10	0.128	1.98	**$<10^{-5}$**	10	0.009	1.914	0.064	10	0.017	3.908	**0.001**
Among individuals within year	449	6.292	97.37	**$<10^{-5}$**	443	0.482	98.64	0.066	399	0.412	95.88	**$<10^{-5}$**

Clustering analyses based on microsatellites performed over the whole dataset revealed three clusters that did not discriminate either years or sites. All voles were assigned to these three

genotypic groups (Fig 4A, B). It is therefore likely that a complete absence of spatio-temporal structure (K = 1) would be the best alternative to explain this result.

Fig 4. STRUCTURE plots of the bank vole metapopulation over the whole survey

The figure presents A) the bar plots resulting from the clustering analysis based on microsatellites and performed for K = 3 on bank voles sampled over the whole survey. Within bar plots, each individual is represented by a single vertical line broken into K colored segments, with lengths proportional to the individual membership coefficients for each individual, in each inferred cluster. Each color represents a different genotypic group. B) The rate of change in the log probability of the data between successive K values ($\Delta(K)$ *i.e.* L"(K) divided by the standard deviation of L(K)) is shown for K = 2 to K = 9.

Spatial autocorrelograms revealed a strong decrease of relatedness between individuals with geographic distance, whatever the sex and year considered (Fig 5). Nevertheless, mean relatedness of females was slightly higher at very small spatial scale (within sampling site or in the first surrounding sites distant from less than 1 km) during peak years (respectively 0.04 and 0.05 in 2005 and 2008) than during the increase phase (0.03 in 2007). In the opposite, relatedness between males was higher within sites during the increase phase (0.03) than during peak years (respectively 0.01 and 0.02 in 2005 and 2008). For each year, the estimates of mean relatedness among seropositive and seronegative voles in the metapopulation showed very low and similar values, respectively r = -0.006 and $r = 6.10^{-4}$ in 2005 (p = 0.344), r = -0.014 and r = -0.006 in 2007 (p = 0.857), r = -0.009 and r = 0.005 in 2008 (p = 0.333) and r = -0.050 and r = 0.030 in 2009 (p = 0.399).

Fig 5. Spatial autocorrelation analyses based on Li's relatedness coefficient.

Correlograms are presented independently for males and females and for each year of sampling between 2005 and 2008. Geographic distances classes are indicated in km. The mean and standard error of Li's relatedness coefficient (78) are indicated for each class.

Detection of signatures of selection

Patterns strongly differed between genes and years, with departures from neutral expectations (i.e. gene heterozygosity and F_{ST} estimates falling outside the envelope that contains 95% or 99% of the simulated data under an island demographic model) being observed in 2007 and 2008 and at immune related SNPs only (Fig 6). In 2007, *Tnf*-296 SNP exhibited high F_{ST} estimates, which could be a signature of positive selection (p = 0.014) and *Tlr4*-1662 SNP showed low F_{ST} estimates, which could indicate balancing selection ($p < 10^{-5}$). In 2008, *Tlr4*-1662 SNP showed high F_{ST} estimates (p = 0.017) and *Mx2*-162 SNP exhibited low F_{ST} estimates ($p = 4 \times 10^{-4}$). No significant departure from neutral expectations was found for *Mhc-Drb*, whatever the year considered (Fig 6).

Fig 6. Detection of signatures of selection at immune related genes (SNPs and *Mhc-Drb*) using Beaumont & Nichols's (1996) approach (Fdist2 program) applied to the whole metapopulation dataset in 2005, 2007 and 2008.

For each year, genetic differentiation indices estimated per locus between sites (single-locus F_{ST} estimates for SNPs in A, B and C and for Mhc-Drb in D, E and F) are plotted against expected heterozygosity (H_e) of the pooled sample. Dark grey, medium grey and light grey areas represent respectively the 90%, 95% and 99% confidence limits simulated under the hypothesis of neutrality. A bi-allelic model has been used in the case of SNPs simulations.

Associations between immune related genotypes and PUUV serology

Immune gene polymorphism marginally discriminated PUUV seropositive and seronegative voles (p = 0.077). Five alleles of the *Mhc-Drb* gene tended to be associated with PUUV serological status. The RR values of Mygl-DRB*106, Mygl-DRB*08 and Mygl-DRB*94 reached respectively 1.724, 1.717 and 1.464, indicating that individuals carrying this allele were almost twice more likely to be PUUV seropositive than others (Fig 7). On the contrary, with a respective RR value of 0.263 and 0.339, bank voles carrying Mygl-DRB*105 and Mygl-DRB*15 were more than twice less likely

to be PUUV seropositive than others (Fig 7). However, after Bonferroni sequential corrections, these RR values were not significant. Note that similar results were observed when considering only over-wintering bank voles that had a long time of potential exposure to PUUV (results not shown).

Fig 7. Discriminant analysis performed on immune related polymorphism of PUUV adult seropositive and PUUV seronegative bank voles over the whole metapopulation.
A) PUUV seropositive adult bank voles, represented by black dot, are marginally different from PUUV-seronegative ones, represented by white dot. B) Alleles indicated in bold (Mygl-DRB*106, Mygl-DRB*08, Mygl-DRB*94, Mygl-DRB*15 and Mygl-DRB*105) are associated with PUUV serological status.

Discussion

In this study, we analysed the genetic variation of a bank vole metapopulation, experiencing three-year population density cycles, at microsatellite loci and immune related genes to examine the potential impact of microevolutionary processes on PUUV epidemiology. Overall, we showed that neutral and adaptive genetic variability was maintained through years despite repeated demographic bottlenecks. Rapid increase in vole density and high gene flow seemed to counterbalance the effects of genetic drift, which may explain the absence of founder effects observed in PUUV populations throughout vole population cycles. Despite this strong influence of demographic processes, selection also participated in driving immune related gene polymorphism. Complex patterns were observed according to the immune related genes and cycle phases considered. Specifically, *Mhc-Drb* polymorphism tended to be associated with PUUV serology, and we found departures from neutral expectations at three other immune related genes with abundance-related patterns, which could reflect signatures of positive and/or balancing selection

Genetic drift, bank vole dispersal and PUUV epidemiology

In boreal Fennoscandia, bank vole populations experience strong multiannual fluctuations in abundance, with peaks occurring every three to five years and abundance varying by a factor 500 between low and peak phases (88). Such regular and severe declines in population size are expected to affect neutral genetic variation through genetic drift. However, several studies have shown that cyclic rodent populations maintained high levels of genetic diversity, at least at a 'metapopulation scale' (10,17,19,20,89,90). Marginal and temporal decreases in allelic richness were previously observed by Rikalainen et al. (18), who studied Finnish bank vole populations at a larger scale (100 km^2) around Konnevesi. Our results provided similar patterns, with high levels of heterozygosity and allelic richness being observed whatever the cycle phase considered. We detected a decrease in allelic richness in the crash phase of 2009 at the scale of the metapopulation. This loss of diversity might be only transient as no decrease could be observed during the increase phase in 2007 that followed the 2006 crash year. Therefore, fluctuations in population size did not lead to strong signature of bottleneck in the genetic data, whatever the spatial scale considered. Similarly, Razzauti et al. (34) did not find any evidence of founder effects affecting PUUV diversity in the area including this vole metapopulation. Significant loss of PUUV variants were detected in 2009 only, with the complete absence of variants from one of the two PUUV genogroups otherwise detected since 2005. These patterns could be explained by the low sampling size in 2009. But it is likely that the low phase is usually too short to impact host genetic diversity, and/or that strong bank vole gene flow might compensate for genetic drift (17). Genetic patterns of temporal and spatial differentiation supported the hypothesis that dispersal among sites may rapidly counterbalance the potential loss of genetic diversity experienced by vole and PUUV populations. Although significant temporal genetic differentiation was locally detected between years, low estimates of temporal genetic differentiation were detected at the scale of the metapopulation. These estimates were slightly higher when comparing pairs of sampling dates before and after decline (especially in 2009). This result corroborated the transient impact of genetic drift on the distribution of genetic variability, and the importance of gene flow occurring after population crash, once vole population size increased again. The relative temporal genetic stability of this metapopulation was also supported by the clustering analysis performed over the whole

survey, as it did not reveal any spatial consistent structuring. Altogether, these results emphasized the absence of environmental heterogeneity within the studied area, typical boreal forest, that could disrupt bank vole gene flow and in turn, PUUV dispersal among sites. The possibility for voles to move all around this area provides an explanation for the absence of spatial structure detected in PUUV population across this area (34).

Spatial autocorrelation analyses enabled to decipher whether population cycles impacted dispersal rate and in turn, PUUV epidemiology. We highlighted changes in the bank vole spatial genetic structure from year to year, that probably resulted from density fluctuations favouring dispersal and population turnover (e.g. 19,20). This raised the question of density-dependent dispersal, that is, whether dispersal rate increased during low phase or with increasing population size (see (92) for references and predictions). As evidenced by Rikalainen et al. (18) and Gauffre et al. (19), our study provided arguments in favour of sex-specific and density-dependence dispersal. Negative density dependent migration of females could underlie the local changes in relatedness observed between low density and peak years. The slightly lower relatedness observed during the increase phase could hence be explained by the colonisation of new empty sites by females. The high levels of relatedness observed during 2005 and 2008 could reflect female phylopatry and low migration (see 93) once population size has reached high abundance. In the opposite, the lower levels of relatedness observed in peak years compared to the increase phase when focusing on males could result from their high dispersal rate and high gene flow once density reached high levels. This sex-biased density dependent migration could be of main importance in shaping PUUV epidemiology. Indeed, a male bias in PUUV infection was detected in Konnevesi only in overwintered, breeding bank voles, whereas a female bias was seen in summer-born breeding animals probably as a result of more frequent contact with old (infected) males or aggressive encounters with other breeding females during the territory establishment (30). In addition, PUUV seropositive voles were found to be more abundant during the high-density years of the dynamic cycle, as confirmed by the strong correlation observed in this study between PUUV seroprevalence and two indices of genetic diversity differentiating peak *versus* low-density years. We could therefore suggest that during low-density phase, female voles could play a role in the

564 colonization of empty sites and consequently in the transmission of PUUV. During peak years,
565 males would be responsible for repeated dispersal events and gene flow, therefore contributing to
566 PUUV transmission.
567

568 Impact of metapopulation dynamics on immune related gene polymorphism

569 Whether natural selection can counterbalance the effect of drift on immune gene polymorphism in
570 populations experiencing drastic fluctuations remains an open research topic, as empirical data
571 have revealed contrasted patterns. From an eco-evolutionary perspective, this question is of
572 uttermost importance as loss of genetic variation could result in dampened adaptive capability,
573 which is especially problematic when faced with rapidly evolving pathogens. A recent meta-
574 analysis showed that a greater loss of genetic diversity was generally seen at *Mhc* genes than at
575 neutral loci, potentially because of the uneven distribution of haplotypes before the bottleneck (7).
576 Here, we studied five genes contributing to immunity, with polymorphism analyzed within protein
577 coding regions (*Mhc-Drb*, *Tlr*s, *Mx2*) or promoter (*Tnf-*α). Variation at these immune related genes
578 has been shown to be associated with rodent responses to PUUV infections (33). Our study first
579 enabled to show the relative role of neutral processes and selection in shaping the geographic
580 variation of immune gene variability in this cyclic bank vole metapopulation. As predicted under
581 genetic drift only, reduction of immune related gene variability was observed at *Mhc-Drb* gene
582 during the crash year 2009, and it was of similar amplitude than the decrease observed at
583 microsatellites. We also noted a particular allele present at low frequencies in one site during the
584 2005 peak year could be lost and never recovered within the metapopulation after the 2006 crash.
585 Such impact of genetic drift was also detected on SNPs, with different patterns detected according
586 to the immune related gene considered. Loss of less frequent variants was for example locally
587 observed after the 2006 crash at *Mx2*_162 SNP only. However, this impact of genetic drift on
588 immune related genes seemed minor and very transient, as there were no such significant
589 temporal changes in allelic frequencies at *Mhc-Drb* or other SNPs. This is in contrast with what
590 was concluded from the meta-analysis of Sutton et al. (7). They proposed that the greater
591 reduction in *Mhc* gene diversity compared to neutral genetic diversity may be observed when

592 negative frequency-dependent selection acting before bottlenecks results in the uneven distribution
593 of most *Mhc* variants/haplotype, what accelerates the loss of *Mhc* variability. Dispersal can be
594 invoked to explain that allelic diversity was recovered once vole abundance increased, as
595 previously seen in Winternitz et al. (10). The detection of previously unseen *Mhc-Drb* haplotypes in
596 particular sites of the metapopulation during the 2008 peak year corroborated this possibility,
597 assuming that it resulted from the immigration of bank voles from outside the metapopulation,
598 carrying these different haplotypes.

599 Further model-based simulations revealed departures from neutrality for several immune
600 related gene polymorphisms. They could reveal complex signatures of balancing or positive
601 selection according to the genes and years / cycle phases considered. A pattern of positive
602 selection was detected at the -296 SNP of *Tnf-α* promoter in 2007 only. *Tnf-α* gene encodes for a
603 cytokine named TNF-α, mediating both acute and chronic inflammatory responses, therefore
604 promoting resistance against a number of infectious agents on one hand. On the other hand, over-
605 production of TNF-α can have important pathological effects and has been associated in humans
606 to the severity of malaria (95) and of hemorrhagic fevers with renal syndrome (96). Changes in the
607 production of this cytokine should hence have important effects on individual fitness (97). We
608 previously showed that polymorphism at the -296 SNP of *Tnf-α* promoter was associated with
609 changes in *Tnf-α* expression levels and susceptibility to PUUV (50,98). As such, this SNP should
610 evolve under strong selection, potentially driven by pathogen mediated pressure and/or energetic
611 trade-offs between costly immunity (pro-inflammatory response) and other costly life history traits.
612 Because of the fine geographical scale of this study, local heterogeneity in pathogen distribution
613 following the 2006 population crash was more likely to lead to spatially varying selection pressure
614 than differences in optimal energetic balance between sites. Higher levels of *Tnf-α* expression
615 could have been favored in sites containing a high diversity of pathogens, or highly virulent ones,
616 as expected in sites C and G in 2007 where frequencies of *Tnf*-296 AA and AG genotypes reached
617 high levels (see 52) for details on genotype/phenotype associations). Inversely, lower levels of *Tnf-*
618 *α* expression could have been selected in sites B and O (high frequencies of GG genotype) if
619 pathogen pressure was weak in 2007. In increase and peak years, bank vole dispersal probably

620 homogenizes these pathogen communities over the whole metapopulation, therefore dampening
621 this directional pathogen-mediated selection.

622 The *Tlr4*-1662 SNP showed signatures of balancing selection in 2007 and positive selection
623 in 2008. *Tlr4* is part of TLRs gene family involved in pathogen recognition (99) and is involved in
624 coevolutionary processes with a wide variety of pathogens (100,101). Several studies recently
625 emphasized the impact of historical and contemporary positive selection on *Tlr4* gene
626 polymorphism in rodents (93,102,103), and it is likely that pathogens might mediate this selection.
627 Again, the signature of positive selection observed in this study might reflect spatial heterogeneity
628 in the whole pathogen community or in one/few pathogens recognized by TLR4. Nevertheless,
629 because positive selection was observed in 2008, a peak year, when gene flow is important during
630 spring when voles mature, and expected to homogenize directly transmitted pathogens, candidates
631 should preferentially be searched among vector-borne agents (e.g. bacteria like *Bartonella* sp.,
632 *Borrelia* sp.) or pathogens able to survive outside their hosts (e.g. ectoparasites). The pattern of
633 balancing selection observed in 2007, the increase year following the bank vole crash, was very
634 similar to what was observed in *Arvicola amphibius* populations after a severe population
635 bottleneck in Scotland (104). Balancing selection mediated by fleas (*Megabothris walkery*), tick
636 larvae (*Ixodes ricinus*) and gamasid mites maintained *Tlr4* genetic diversity in this isolated water
637 vole population.

638 Patterns of balancing selection were also observed at *Mx2* gene, although a significant
639 signature was only detected in 2008. *Mx2* gene encodes for proteins that provide immunity against
640 viruses replicating in the cytoplasm, including hantaviruses (105,106). The SNP detected under
641 selection was located within the leucine zipper motif of the C-terminal GTP effector domain, where
642 mutations can affect the antiviral efficacy of Mx proteins (107–109). Balancing selection could be
643 mediated by spatio-temporal heterogeneity in candidate viruses, and it would be stronger during
644 peak year when dispersal may homogenize their distribution within the area. We previously
645 showed that the levels of *Mx2* gene expression were negatively correlated with PUUV prevalence
646 in France (98). It would therefore be interesting to analyze whether different *Mx2* haplotypes have

different efficacies in recognizing the various PUUV genogroups (including reassortants, see 33) circulating around Konnevesi.

Such diversity of patterns has previously been described in arvicoline rodents experiencing population cycles. Bryja et al. (14) found density-dependent changes in selection pressure throughout a complete density cycle of the montane water vole (*Arvicola scherman*), and these changes were detected at only one *Mhc* class II gene over the two examined. In cyclic populations of field vole (*Microtus agrestis*), Turner et al. (93) detected signature of selection acting on only two genes encoding cytokines over the twelve immune related genes examined. This variability in observed patterns could be mediated by different pathogens affecting different parts of the genome and temporal heterogeneity in pathogen pressure (e.g. 95) that can have a strong selective effect of selection even in a few generations (e.g. 11). Nevertheless, we have to take these results cautiously as the statistical tests applied to detect selection are based on an equilibrium island model, so that a number of assumptions are violated in this study (non-equilibrium population dynamics, spatial autocorrelations reflecting potential isolation by distance). Integrating a more realistic demographic model of population structure and historical demography could help corroborating the impact of selection on the observed patterns of SNP frequencies.

Conclusions

This study provides evidence of contemporary selection acting on immune related genes in rodent populations experiencing marked three-year population cycles. Although we can only speculate about the potential influence of pathogens as drivers of this selection, it is likely that these adaptive changes may affect *M. glareolus* / PUUV interactions, either directly (these immune related genes are known to impact host responses to PUUV infection) or indirectly via the role of coinfection on PUUV epidemiology (98,110). PUUV should therefore not only evolve under neutral microevolutionary processes in this area. In the future, combining such population genetics approaches at neutral and immune related genes with high-throughput characterization of rodent microbial communities should offer new opportunities to better understand rodent/hantavirus interactions.

675

676 **Supporting Information**

677 **S1 Protocol:** SNPs identification and genotyping

678 **S1 Table**: Characteristics and genetic diversity estimates within each year and each sampling site,
679 including the number of bank voles sampled (N) and PUUV positives (Ni), PUUV seroprevalence
680 and the genetic diversity estimates (H_o, H_e, F_{IS}, N_a). When less than eight individuals were sampled
681 in a site, local estimates were not calculated (- and all the sites in 2009). 'Total' refers to the whole
682 metapopulation. Significant values are in bold.

683 **S2 Table**: Primers used for *M. glareolus* identification, amplification of gDNA for PCR and
684 sequencing with corresponding fragment length and total length of the sequence.

685 **S3 Table:** Cycling conditions of PCRs.

686 **S4 Table**: Results of the two linear miwed models. Only significant pairwise interactions are
687 reported.

688 **S5 Table**: F_{ST} estimates between sites per year (lower side) and associated *p*-values of Fisher
689 exact tests (upper side).

690 **S6 Table.** F_{ST} estimates between years over the whole metapopulation (lower side) and associated
691 *p*-values of Fisher exact tests (upper side).

692 **S7 Table:** This file includes a) the individual and spatial data of all bank voles, b) the microsatellite
693 genotypes for 19 loci, c) the genotypic data for four immune related genes (4 independent SNPs
694 genotyped using the KASPar technology) and d) the Mhc-Drb exon 2 genotypes (sequences are
695 available in Genbank).

696

697 **Acknowledgments**

698 Microsatellite data used in this work were produced through the technical facilities of the Centre
699 Méditerranéen Environnement Biodiversité (CeMEB). We are grateful to Audrey Rohfritsch and
700 Viola Walther for the identification of SNPs at immune gene during the pilot study. We are grateful
701 to Jeremy Gaudin for technical assistance and preliminary analyses.

702

703 **Fundings**

This research has been partially funded by EU grants GOCE-CT-2003- 010284 EDEN and FP7-261504 EDENext, and the paper is catalogued by the EDENext Steering Committee as EDENext 405 (http://www.edenext.eu). AD is currently funded by an INRA-EFPA / ANSES fellowship.

Author Contributions

Conceived and designed the vole sampling survey, analyzed PUUV serology: HH, JN, MR, LV. Conceived and designed the molecular analyses: AD, MG, JFC, EG, NC. Analyzed the data: AD, BG, RV, EG. Wrote the paper: AD, NC, BG, RV. LV, HH, MR and JFC helped to improve and draft the manuscript. All authors have read and approved the final manuscript.

References

1. Archie E a, Luikart G, Ezenwa VO. Infecting epidemiology with genetics: a new frontier in disease ecology. Trends Ecol Evol. 2009;24(1):21–30.
2. Price PW. Evolutionary biology of parasites (Vol. 15). Princeton University Press; 1980. 237 p.
3. Biek R, Real L. The landscape genetics of infectious disease emergence and spread. Mol Ecol. 2010;19(17):3515–31.
4. Cullingham CI, Kyle CJ, Pond BA, Rees EE, White BN. Differential permeability of rivers to raccoon gene flow corresponds to rabies incidence in Ontario, Canada. Mol Ecol. 2009;18(1):43–53.
5. Charbonnel N, Cosson J-F. Molecular Epidemiology of Disease Resistance Genes with Perspectives for Researches on Biological Invasions and Hybrid Zones. In: S M, Beaudeau F, Cabaret J, de Rycke J, editors. New Frontiers of Molecular Epidemiology of Infectious Diseases. Dordrecht: Springer Netherlands; 2011. p. 255–90.
6. Ejsmond MJ, Radwan J. MHC diversity in bottlenecked populations: a simulation model. Conserv Genet. 2011;12(1):129–37.
7. Sutton JT, Nakagawa S, Robertson BC, Jamieson IG. Disentangling the roles of natural selection and genetic drift in shaping variation at MHC immunity genes. Mol Ecol. 2011;20(21):4408–20.

8. Grueber CE, Wallis GP, Jamieson IG. Genetic drift outweighs natural selection at toll-like receptor (TLR) immunity loci in a re-introduced population of a threatened species. Mol Ecol. 2013;22(17):4470–82.

9. Oliver MK, Piertney SB. Selection maintains MHC diversity through a natural population bottleneck. Mol Biol Evol. 2012;29(7):1713–20.

10. Winternitz JC, Wares JP, Yabsley MJ, Altizer S. Wild cyclic voles maintain high neutral and MHC diversity without strong evidence for parasite-mediated selection. Evol Ecol. 2014;28:957–75.

11. Frankham R. Effective population size/adult population size ratios in wildlife: a review. Genet Res. 1995;66(2):95–107.

12. Nei M, Maruyama T, Chakraborty R. The bottleneck effect and genetic variability in populations. Evolution. 1975;29:1–10.

13. Maruyama T, Fuerst PA. Population bottlenecks and nonequilibrium models in population genetics. II. Number of alleles in a small population that was formed by a recent bottleneck. Genetics. 1985;111:675–89.

14. Bryja J, Charbonnel N, Berthier K, Galan M, Cosson JF. Density-related changes in selection pattern for major histocompatibility complex genes in fluctuating populations of voles. Mol Ecol. 2007;16:5084–97.

15. Burton C, Krebs CJ, Taylor EB. Population genetic structure of the cyclic snowshoe hare (*Lepus americanus*) in southwestern Yukon, Canada. Mol Ecol. 2002;11:1689–701.

16. Berthier K, Charbonnel N, Galan M, Chaval Y, Cosson J-F. Migration and recovery of the genetic diversity during the increasing density phase in cyclic vole populations. Mol Ecol. 2006;15:2665–76.

17. Ehrich D, Yoccoz NG, Ims RA. Multi-annual density fluctuations and habitat size enhance genetic variability in two northern voles. Oikos. 2009;118(10):1441–52.

18. Rikalainen K, Aspi J, Galarza J a, Koskela E, Mappes T. Maintenance of genetic diversity in cyclic populations-a longitudinal analysis in *Myodes glareolus*. Ecol Evol. 2012;2(7):1491–502.

19. Gauffre B, Berthier K, Inchausti P, Chaval Y, Bretagnolle V, Cosson JF. Short-term variations in gene flow related to cyclic density fluctuations in the common vole. Mol Ecol. 2014;23:3214–25.

762 20. Berthier K, Galan M, Foltête JC, Charbonnel N, Cosson JF. Genetic structure of the cyclic
763 fossorial water vole (*Arvicola terrestris*): landscape and demographic influences. Mol Ecol.
764 2005;14(9):2861–71.

765 21. Hanski I, Henttonen H. Population cycles of small rodents in Fennoscandia. In: Berryman A,
766 editor. Populations cycles: the case for trophic interactions. 2002. p. 44–68.

767 22. Henttonen H, McGuire AD, Hansson L. Spectral analyses on density variations. Ann. Zool.
768 Fennici. 1985. p. 221–7.

769 23. Vaheri A, Henttonen H, Voutilainen L, Mustonen J, Sironen T, Vapalahti O. Hantavirus
770 infections in Europe and their impact on public health. Rev Med Virol Virol. 2012;23(1):35–49.

771 24. Voutilainen L, Sironen T, Tonteri E, Tuiskunen Back A, Razzauti M, Karlsson M, et al. Life-
772 Long Shedding of Puumala Hantavirus in Wild Bank Voles (*Myodes glareolus*). J Gen Virol.
773 2015;96(6):1438–47.

774 25. Bernshtein AD, Apekina NS, Mikhailova T V., Myasnikov YA, Khlyap LA, Korotkov YS, et al.
775 Dynamics of Puumala hantavirus infection in naturally infected bank voles (*Clethrinomys*
776 *glareolus*). Arch Virol. 1999;144(12):2415–28.

777 26. Meyer BJ, Schmaljohn CS. Persistent hantavirus infections: characteristics and
778 mechanisms. Trends Microbiol. 2000;8(2):61–7.

779 27. Kallio ER, Voutilainen L, Vapalahti O, Vaheri A, Henttonen H, Koskela E, et al. Endemic
780 hantavirus infection impairs the winter survival of its rodent host. Ecology. 2007;88(8):1911–6.

781 28. Kallio ER, Helle H, Koskela E, Mappes T, Vapalahti O. Age-related effects of chronic
782 hantavirus infection on female host fecundity. J Anim Ecol. 2015;84(5):1264–72.

783 29. Tersago K, Crespin L, Verhagen R, Leirs H. Impact of Puumala virus infection on maturation
784 and survival in bank voles: a capture-mark-recapture analysis. J Wildl Dis. 2012;48(1):148–56.

785 30. Voutilainen L, Kallio ER, Niemimaa J, Vapalahti O, Henttonen H. Temporal dynamics of
786 Puumala hantavirus infection in cyclic populations of bank voles. Sci Rep. 2016.

787 31. Guivier E, Galan M, Chaval Y, Xuéreb A, Ribas Salvador A, Poulle M-L, et al. Landscape
788 genetics highlights the role of bank vole metapopulation dynamics in the epidemiology of
789 Puumala hantavirus. Mol Ecol. 2011;20(17):3569–83.

790 32. Weber de Melo V, Sheikh Ali H, Freise J, Kühnert D, Essbauer S, Mertens M, et al.
791 Spatiotemporal dynamics of Puumala hantavirus associated with its rodent host, *Myodes*
792 *glareolus*. Evol Appl. 2015;8(6):545–59.

793 33. Charbonnel N, Pagès M, Sironen T, Henttonen H, Vapalahti O, Mustonen J, et al.
794 Immunogenetic factors affecting susceptibility of humans and rodents to hantaviruses and the
795 clinical course of hantaviral disease in humans. Viruses. 2014;6(5):2214–41.

796 34. Razzauti M, Plyusnina A, Henttonen H, Plyusnin A. Microevolution of Puumala hantavirus
797 during a complete population cycle of its host, the bank vole (*Myodes glareolus*). PLoS One.
798 2013;8(5):e64447.

799 35. Deter J, Chaval Y, Galan M, Gauffre B, Morand S, Henttonen H, et al. Kinship, dispersal
800 and hantavirus transmission in bank and common voles. Arch Virol. 2008;153(3):435–44.

801 36. Razzauti M, Plyusnina A, Sironen T, Henttonen H, Plyusnin A. Analysis of Puumala
802 hantavirus in a bank vole population in northern Finland: evidence for co-circulation of two
803 genetic lineages and frequent reassortment between strains. J Gen Virol. 2009;90(8):1923–31.

804 37. Kallio-Kokko H, Laakkonen J, Rizzoli a, Tagliapietra V, Cattadori I, Perkins SE, et al.
805 Hantavirus and arenavirus antibody prevalence in rodents and humans in Trentino, Northern
806 Italy. Epidemiol Infect. 2006;134(4):830–6.

807 38. Voutilainen L. Interactions between Puumala hantavirus and its host, the bank vole, in the
808 boreal zone. 2013.

809 39. Razzauti M, Plyusnina A, Henttonen H, Plyusnin A. Accumulation of point mutations and
810 reassortment of genomic RNA segments are involved in the microevolution of Puumala
811 hantavirus in a bank vole (*Myodes glareolus*) population. J Gen Virol. 2008;89(7):1649–60.

812 40. Kallio ER, Poikonen A, Vaheri A, Vapalahti O, Henttonen H, Koskela E, et al. Maternal
813 antibodies postpone hantavirus infection and enhance individual breeding success. Proc Roy S
814 Lond.2006;(273):2771–6.

815 41. Hardestam J, Karlsson M, Falk KI, Olsson G, Klingström J, Lundkvist A. Puumala
816 hantavirus excretion kinetics in bank voles (*Myodes glareolus*). Emerg Infect Dis.
817 2008;14(8):1209–15.

818 42. Rikalainen K, Grapputo a, Knott E, Koskela E, Mappes T. A large panel of novel
819 microsatellite markers for the bank vole (*Myodes glareolus*). Mol Ecol Resour. 2008;8(5):1164–
820 8.

821 43. Rohfritsch A, Guivier E, Galan M, Chaval Y, Cosson J-F, Charbonnel N. Apport de
822 l'immunogénétique à la compréhension des interations entre le campagnol roussâtre *Myodes*
823 *glareolus* et l'hantavirus Puumala. Bull Acad Vet Fr. Académie vétérinaire de France;
824 2013;166(2):171–83.

825 44. Kloch A, Babik W, Bajer A, Siński E, Radwan J. Effects of an MHC-DRB genotype and
826 allele number on the load of gut parasites in the bank vole *Myodes glareolus*. Mol Ecol. 2010;19
827 Suppl 1:255–65.

828 45. Ayres JS, Schneider DS. Tolerance of infections. Annu Rev Immunol. 2012;30:271–94.

829 46. Wlasiuk G, Nachman MW. Adaptation and constraint at toll-like receptors in primates. Mol
830 Biol Evol. 2010;27(9):2172–86.

831 47. Sabeti PC, Varilly P, Fry B, Lohmueller J, Hostetter E, Cotsapas C, et al. Genome-wide
832 detection and characterization of positive selection in human populations. Nature.
833 2007;449(7164):913–8.

834 48. Bowie AG, Haga IR. The role of Toll-like receptors in the host response to viruses. Mol
835 Immunol. 2005;42(8):859–67.

836 49. Vassalli P. The pathophysiology of Tumor Necrosis Factor. Annu Rev Immunol.
837 1992;10:411–52.

838 50. Guivier E, Galan M, Salvador AR, Xuéreb A, Chaval Y, Olsson GE, et al. Tnf-α expression
839 and promoter sequences reflect the balance of tolerance/resistance to Puumala hantavirus
840 infection in European bank vole populations. Infect Genet Evol. 2010;10(8):1208–17.

841 51. Bouma G, Crusius JB, Oudkerk Pool M, Kolkman JJ, von Blomberg BM, Kostense PJ, et al.
842 Secretion of tumour necrosis factor alpha and lymphotoxin alpha in relation to polymorphisms in
843 the Tnf genes and Hla-Dr alleles. Relevance for inflammatory bowel disease. Scand J Immunol.
844 1996;43(4):456–63.

845 52. Wilson a G, Symons J a, McDowell TL, McDevitt HO, Duff GW. Effects of a polymorphism
846 in the human tumor necrosis factor alpha promoter on transcriptional activation. Proc Natl Acad
847 Sci U S A. 1997;94(7):3195–9.

848 53. Jin HK, Takada a, Kon Y, Haller O, Watanabe T. Identification of the murine Mx2 gene:
849 interferon-induced expression of the Mx2 protein from the feral mouse gene confers resistance
850 to vesicular stomatitis virus. J Virol. 1999;73(6):4925–30.

851 54. Porter BF, Ambrus a, Storts RW. Immunohistochemical evaluation of mx protein expression
852 in canine encephalitides. Vet Pathol. 2006;43(6):981–7.

853 55. Galan M, Guivier E, Caraux G, Charbonnel N, Cosson J-F. A 454 multiplex sequencing
854 method for rapid and reliable genotyping of highly polymorphic genes in large-scale studies.
855 BMC Genomics. 2010;11:296.

856 56. Schad J, Sommer S, Ganzhorn JU. MHC Variability of a Small Lemur in the Littoral Forest
857 Fragments of Southeastern Madagascar. Conserv Genet. 2004;5(3):299–309.

858 57. Galan M, Pagès M, Cosson J-F. Next-generation sequencing for rodent barcoding: species
859 identification from fresh, degraded and environmental samples. PLoS One. 2012;7(11).

860 58. Piry S, Guivier E, Realini a, Martin J-F. SESAME Barcode: NGS-oriented software for
861 amplicon characterization--application to species and environmental barcoding. Mol Ecol
862 Resour. 2012;12(6):1151–7.

863 59. Hall TA. BioEdit: a user-friendly biological sequence alignment editor and analysis program
864 for Windows 95/98/NT. Nucleic Acids Symposium Series. 1999. p. 95–8.

865 60. Chenna R, Sugawara H, Koike T, Lopez R, Gibson TJ, Higgins DG, et al. Multiple sequence
866 alignment with the Clustal series of programs. Nucleic Acids Res. 2003;31(13):3497–500.

867 61. Klein J, Bontrop RE, Dawkins RL, Erlich HA, Gyllensten UB, Heise ER, et al. Nomenclature
868 for the major histocompatibility complexes of different species: a proposal. The HLA System in
869 Clinical Transplantation. Springer Berlin Heidelberg.; 1993. p. 407–11.

870 62. Tamura K, Dudley J, Nei M, Kumar S. MEGA4: Molecular Evolutionary Genetics Analysis
871 (MEGA) software version 4.0. Mol Biol Evol. 2007;24(8):1596–9.

872 63. Axtner J, Sommer S. Gene duplication, allelic diversity, selection processes and adaptive
873 value of MHC class II DRB genes of the bank vole, *Clethrionomys glareolus*. Immunogenetics.
874 2007;59(5):417–26.

875 64. Raymond M, Rousset F. An exact test for population differentiation. Evolution.
876 1995;49(6):1283–1283.

877 65. Benjamini Y, Hochberg Y. Controlling the False Discovery Rate : A Practical and Powerful
878 Approach to Multiple Testing. J R Stat Soc. 1995;57(1):289–300.

879 66. Goudet J. FSTAT (version 1.2): a computer program to cal culate *F*-statistics. J Hered.
880 1995;86:485–6.

881 67. El Mousadik A, Petit R. High level of genetic differentiation for allelic richness among
882 populations of the argan tree [*Argania spinosa* (L.) Skeels] endemic to Morocco. Theor Appl
883 Genet. 1996;92:832–9.

884 68. Nei M. Estimation of average heterozygosity and genetic distance from a small number of
885 individuals. Genetics. 1978;89(3):583–90.

886 69. Weir B., Cockerham C. Estimating F-statistics for the analysis of population structure.
887 Evolution. 1984;38(6):1358–70.

888 70. Belkhir K, Borsa P, Chikhi L, Raufaste N, Bonhomme F. GENETIX 4.05, logiciel sous
889 Windows TM pour la génétique des populations. 1996. Laboratoire génome, populations,
890 interactions, CNR.

891 71. R Core Team. R: A language and environment for statistical computing. 2013.

892 72. Foll M, Gaggiotti O. Identifying the Environmental Factors That Determine the Genetic
893 Structure of Populations. Genetics. 2006;174(2):875–91.

894 73. Excoffier L, Lischer HEL. Arlequin suite ver 3.5: a new series of programs to perform
895 population genetics analyses under Linux and Windows. Mol Ecol Resour. 2010;10(3):564–7.

896 74. Pritchard JK, Stephens M, Donnelly P. Inference of population structure using multilocus
897 genotype data. Genetics. 2000;155(2):945–59.

898 75. Evanno G, Regnaut S, Goudet J. Detecting the number of clusters of individuals using the
899 software STRUCTURE: a simulation study. Mol Ecol. 2005;14(8):2611–20.

900 76. Jakobsson M, Rosenberg N a. CLUMPP: a cluster matching and permutation program for
901 dealing with label switching and multimodality in analysis of population structure. Bioinformatics.
902 2007;23(14):1801–6.

903 77. Rosenberg NA. Distruct : a program for the graphical display of population structure. 2007.

904 78. Li CC, Weeks DE, Chakravarti A. Similarity of DNA finger prints due to chance and
905 relatedness. Hum Hered. 1993;43:45–52.

906 79. Hardy O, Vekemans X. SPAGeDi: a versatile computer program to analyse spatial genetic
907 structure at the individual or population levels. Mol Ecol Notes. 2002;2:618–20.

908 80. Vekemans X, Hardy OJ. New insights from fine-scale spatial genetic structure analyses in
909 plant populations. Mol Ecol. 2004;13(4):921–35.

910 81. Prugnolle F, Meeûs T De. Inferring sex-biased dispersal from population genetic tools: a
911 review. Heredity 2002;161–5.

912 82. Coulon A, Cosson J-F, Morellet N, Angibault J-M, Cargnelutti B, Galan M, et al. Dispersal is
913 not female biased in a resource-defence mating ungulate, the European roe deer. Proc Biol Sci.
914 2006;273(1584):341–8.

915 83. Hansson L. Geographic differences in the sociability of voles in relation to cyclicity. Anim
916 Behav. 1986;34(4):1215–21.

917 84. Beaumont M a., Nichols R a. Evaluating Loci for Use in the Genetic Analysis of Population
918 Structure. Proc R Soc B Biol Sci. 1996;263(1377):1619–26.

919 85. Beaumont MA. Adaptation and speciation: What can F_{ST} tell us? Trends Ecol Evol.
920 2005;20(8):435–40.

921 86. Thioulouse J, Chessel D, Dolédec S, Olivier J. ADE-4: a multivariate analysis and graphical
922 display software. Stat Comput. 1997;7:75–83.

923 87. Haldane BJ. The estimation and significance of the logarithm of a ratio of frequencies. Ann
924 Hum Genet. 1956;20(4):309–11.

925 88. Hansson B, Henttonen H. Rodent dynamics as community processes. Trends Ecol Evol.
926 1988;8:195–200.

927 89. Ehrich D, Jorde PE, Krebs CJ, Kenney a J, Stacy JE, Stenseth NC. Spatial structure of
928 lemming populations (*Dicrostonyx groenlandicus*) fluctuating in density. Mol Ecol.
929 2001;10(2):481–95.

930 90. García-Navas V, Bonnet T, Waldvogel D, Wandeler P, Camenisch G, Postma E. Gene flow
931 counteracts the effect of drift in a Swiss population of snow voles fluctuating in size. Biol
932 Conserv. Elsevier B.V.; 2015;191:168–77.

933 91. Pilot M, Dąbrowski MJ, Jancewicz E, Schtickzelle N, Gliwicz J. Temporally stable genetic
934 variability and dynamic kinship structure in a fluctuating population of the root vole Microtus
935 oeconomus. Mol Ecol. 2010;19:2800–12.

936 92. Le Galliard J, Rémy A, Ims R, Lambin X. Patterns and processes of dispersal behaviour in
937 arvicoline rodents. Mol Ecol. 2012;21:505–23.

938 93. Turner AK, Begon M, Jackson J a., Paterson S. Evidence for selection at cytokine loci in a
939 natural population of field voles (*Microtus agrestis*). Mol Ecol. 2012;21(7):1632–46.

940 94. Fraser B, Ramnarine I, Neff B. Temporal variation at the Mhc class IIB in wild populations of
941 the guppy (*Poecilia reticulata*). Evolution. 2010;64:2086–96.

942 95. Kwiatkowski D, Hill a V, Sambou I, Twumasi P, Castracane J, Manogue KR, et al. TNF
943 concentration in fatal cerebral, non-fatal cerebral, and uncomplicated *Plasmodium falciparum*
944 malaria. Lancet. 1990;336(8725):1201–4.

945 96. Klingstrom J, Plyusnin A, Vaheri A, Lundkvist A. Wild-type Puumala hantavirus infection
946 induces cytokines, C-reactive protein, creatinine, and nitric oxide in cynomolgus macaques. J
947 Virol. 2002;76(1):444–9.

948 97. Knight JC, Kwiatkowski D. Inherited variability of tumor necrosis factor production and
949 susceptibility to infectious disease. Proc Assoc Am Physicians. 1999;111(4):290–8.

950 98. Guivier E, Galan M, Henttonen H, Cosson J-F, Charbonnel N. Landscape features and
951 helminth co-infection shape bank vole immunoheterogeneity, with consequences for Puumala
952 virus epidemiology. Heredity; 2014;112(3):274–81.

953 99. Kawai T, Akira S. Pathogen recognition with Toll-like receptors. Curr Opin Immunol.
954 2005;17(4):338–44.

955 100. Akira S, Uematsu S, Takeuchi O. Pathogen recognition and innate immunity. Cell.
956 2006;124(4):783–801.

957 101. Hughes AL, Piontkivska H. Functional diversification of the toll-like receptor gene family.
958 Immunogenetics. 2008;60(5):249–56.

959 102. Fornůsková A, Bryja J, Vinkler M, Macholán M, Piálek J. Contrasting patterns of
960 polymorphism and selection in bacterial-sensing toll-like receptor 4 in two house mouse
961 subspecies. Ecol Evol. 2014;4(14):2931–44.

962 103. Fornůsková A, Vinkler M, Pagès M, Galan M, Jousselin E, Cerqueira F, et al. Contrasted
963 evolutionary histories of two Toll-like receptors (Tlr4 and Tlr7) in wild rodents (Murinae). BMC
964 Evol Biol. 2013;13:194.

965 104. Gavan MK, Oliver MK, Douglas A, Piertney SB. Gene dynamics of toll-like receptor 4
966 through a population bottleneck in an insular population of water voles (*Arvicola amphibius*).
967 Conserv Genet. 2015;16(5):1181–93.

968 105. Jin HK, Yoshimatsu K, Takada A, Ogino M, Asano A, Arikawa J, et al. Mouse Mx2 protein
969 inhibits hantavirus but not influenza virus replication. Arch Virol. 2001;146(1):41–9.

970 106. Lee SH, Vidal SM. Functional diversity of Mx proteins: Variations on a theme of host
971 resistance to infection. Genome Res. 2002;12(4):527–30.

972 107. Janzen C, Kochs G, Haller O. A monomeric GTPase-negative MxA mutant with antiviral
973 activity. J Virol. 2000;74(17):8202–6.

974 108. Kochs G, Haller O. Interferon-induced human MxA GTPase blocks nuclear import of
975 Thogoto virus nucleocapsids. Proc Natl Acad Sci. 1999;96(5):2082–6.

109. Zürcher T, Pavlovic J, Staeheli P. Mechanism of human MxA protein action: variants with changed antiviral properties. EMBO J. 1992;11(4):1657–61.

110. Ribas Salvador A, Guivier E, Xuéreb A, Chaval Y, Cadet P, Poulle M-L, et al. Concomitant influence of helminth infection and landscape on the distribution of Puumala hantavirus in its reservoir, *Myodes glareolus*. BMC Microbiol; 2011;11(1):30.

111. Thompson JD, Higgins DG, Gibson TJ. CLUSTAL W: improving the sensitivity of progressive multiple sequence alignment through sequence weighting, position-specific gap

A

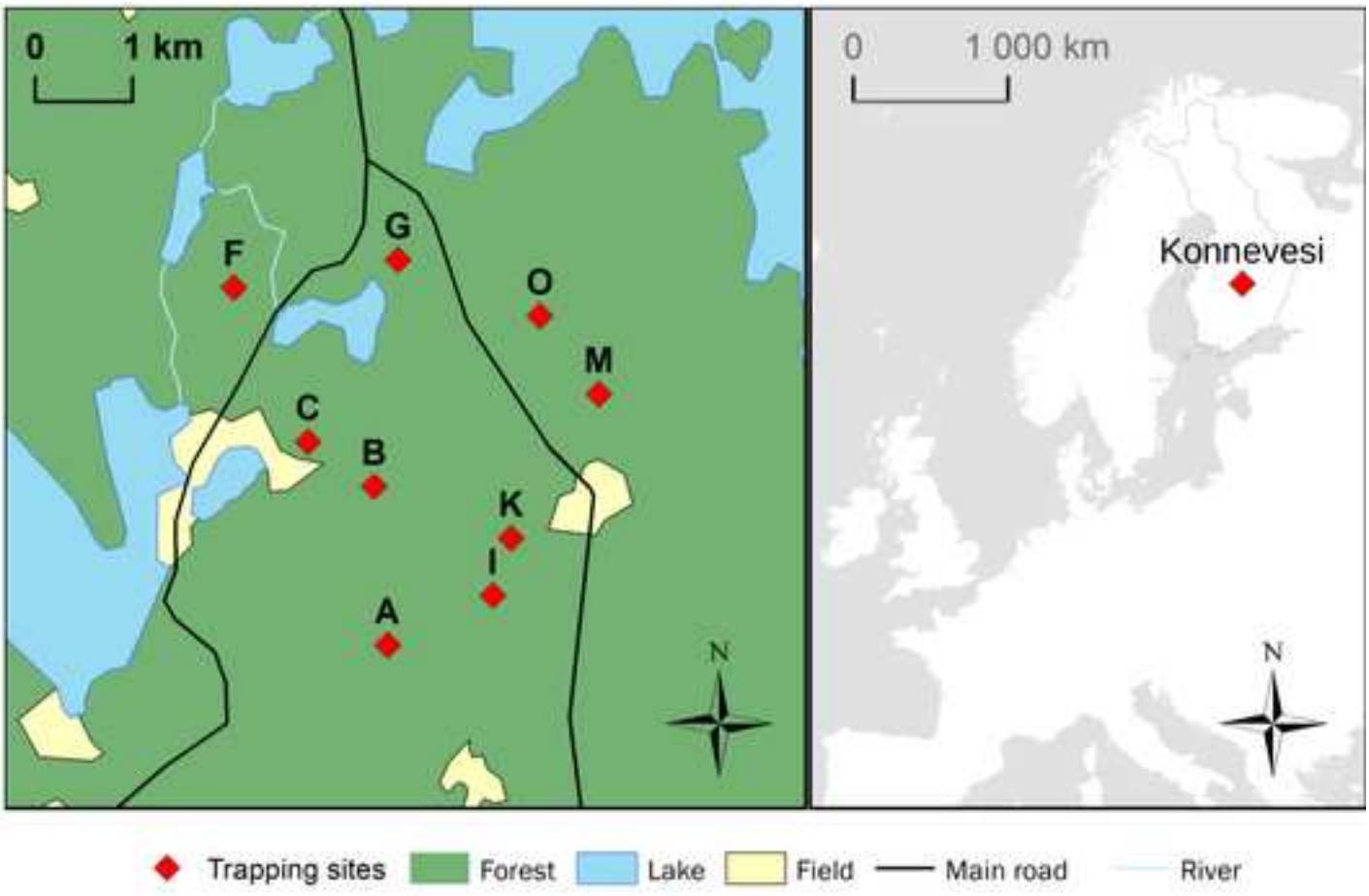
0 1 km
F
G
O
M
C
B
K
I
A
N
0 1 000 km
Konnevesi
N
Trapping sites
Forest
Lake
Field
Main road
River

B

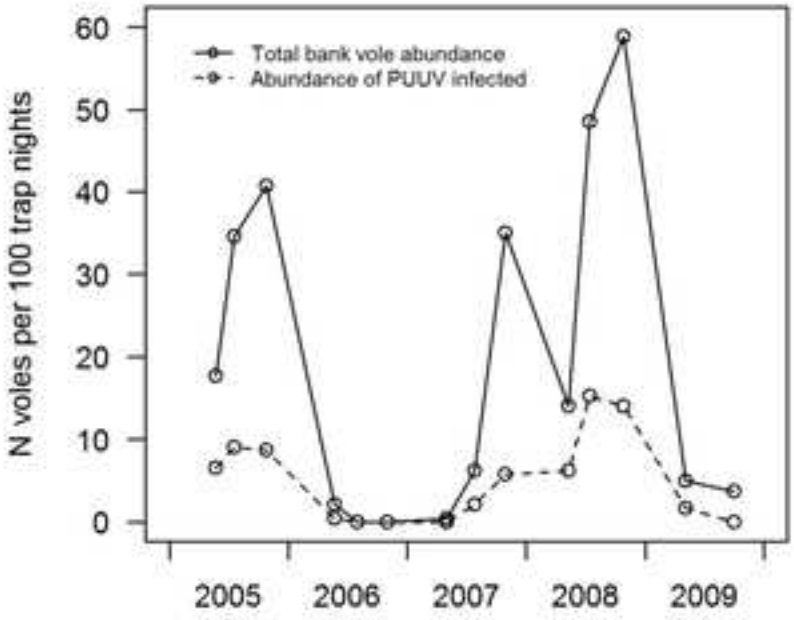
Total bank vole abundance
Abundance of PUUV infected
N voles per 100 trap nights
60
50
40
30
20
10
0
2005
2006
2007
2008
2009

Figure2

Click here to download Figure Figure2_Dubois.tiff

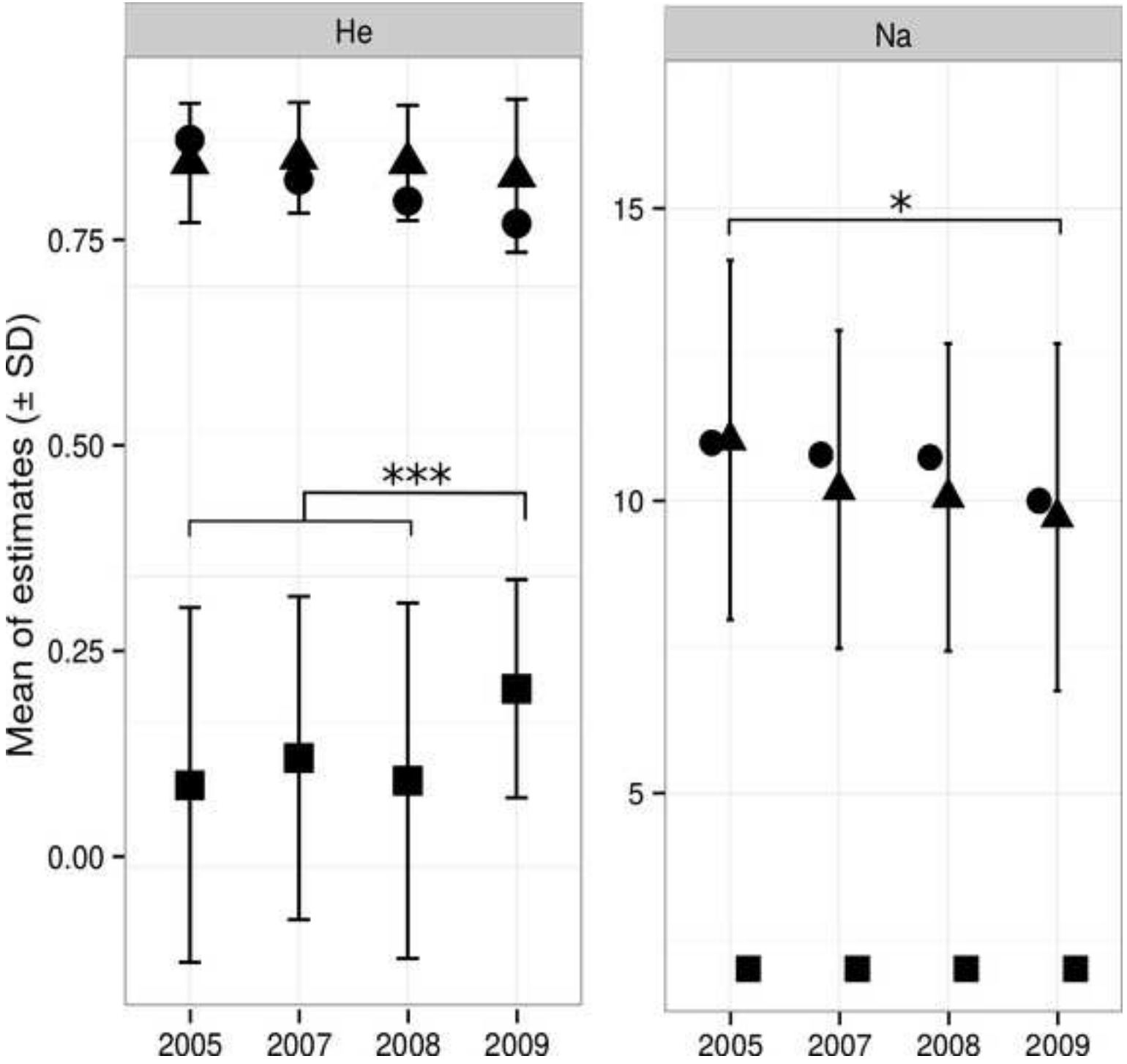

Figure3

Click here to download Figure Figure3_Dubois.tiff

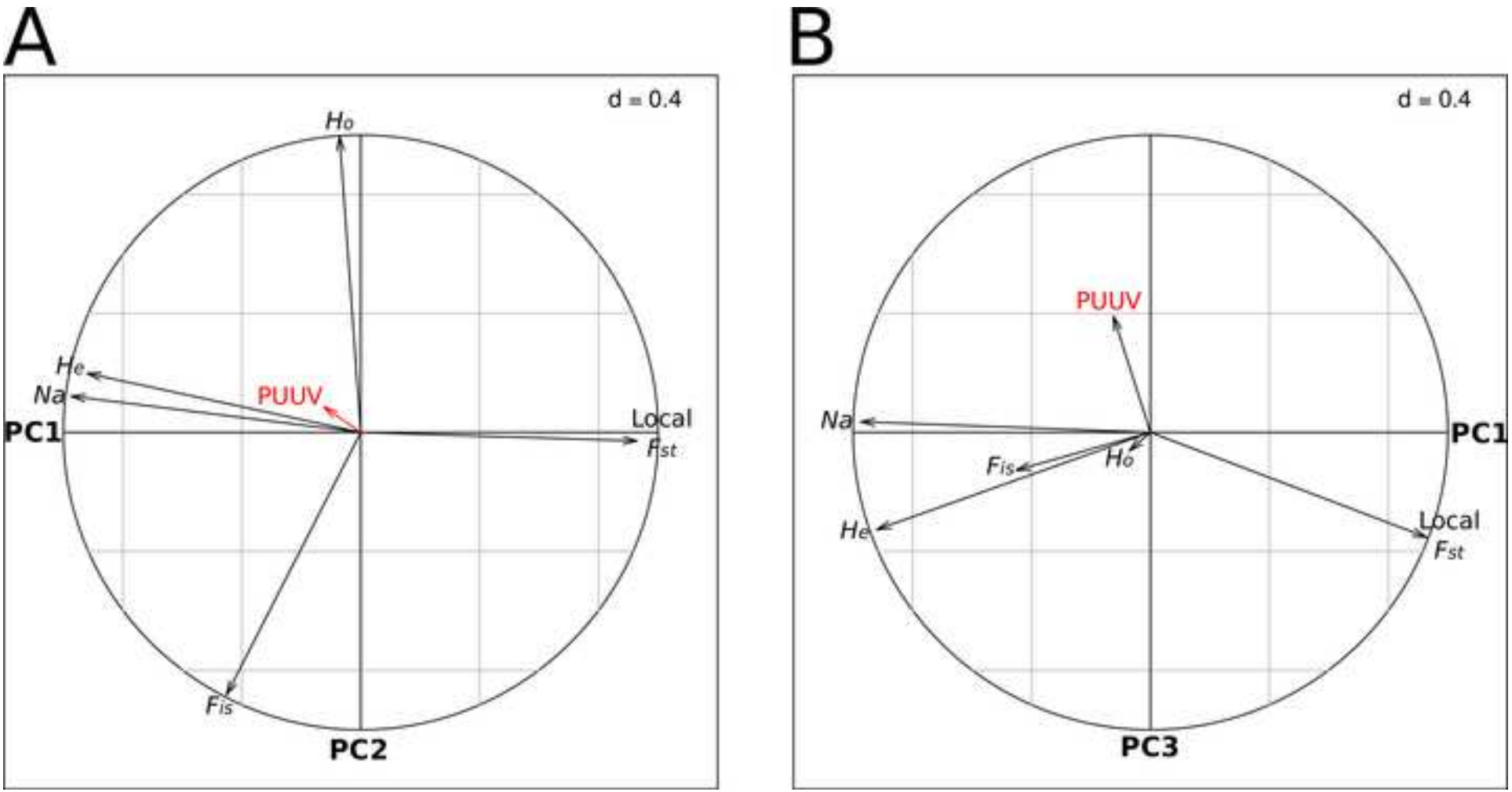

Figure4

Click here to download Figure Figure4_Dubois.tiff

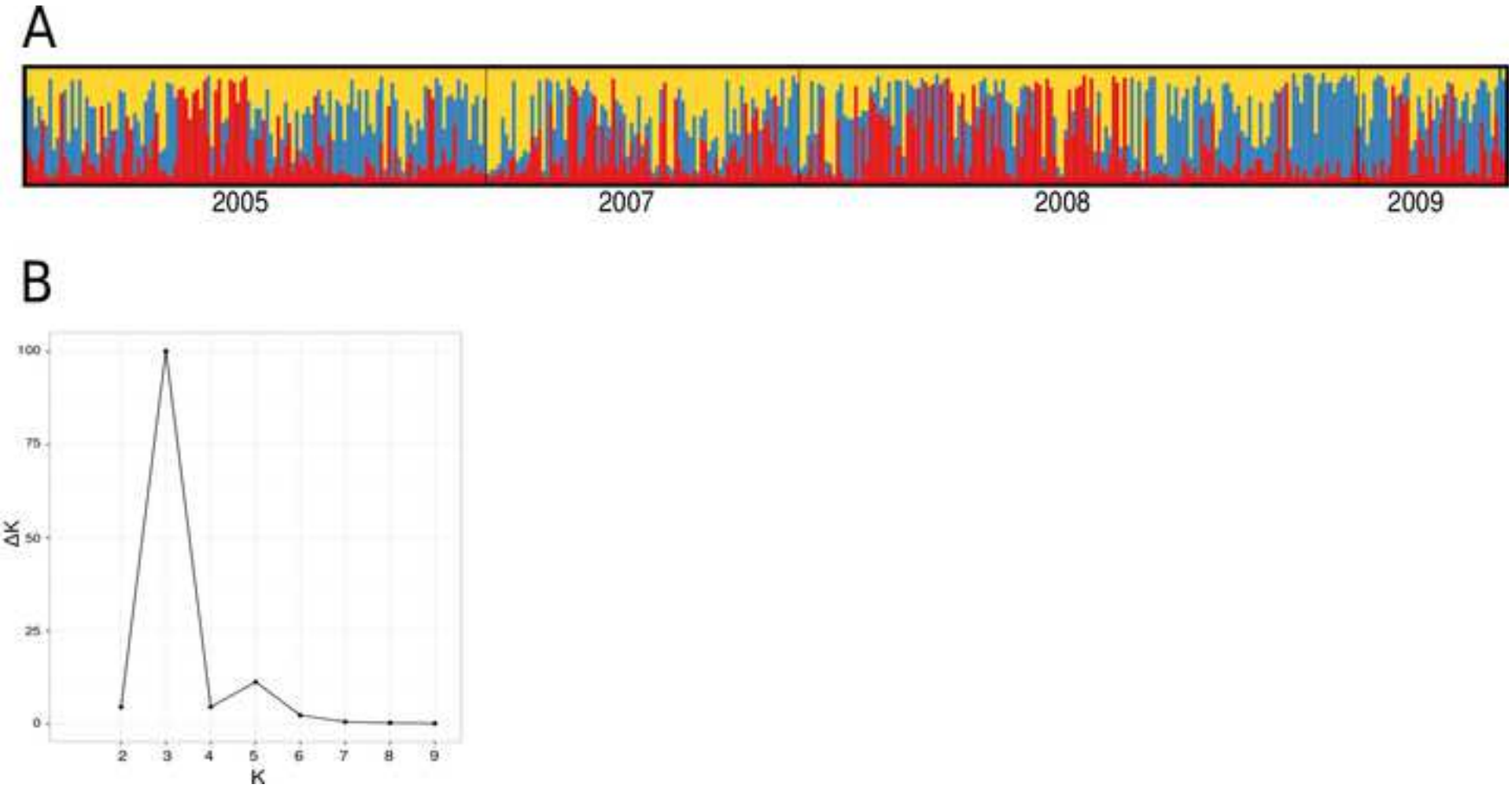

Figure5

Click here to download Figure Figure5_Dubois.tiff

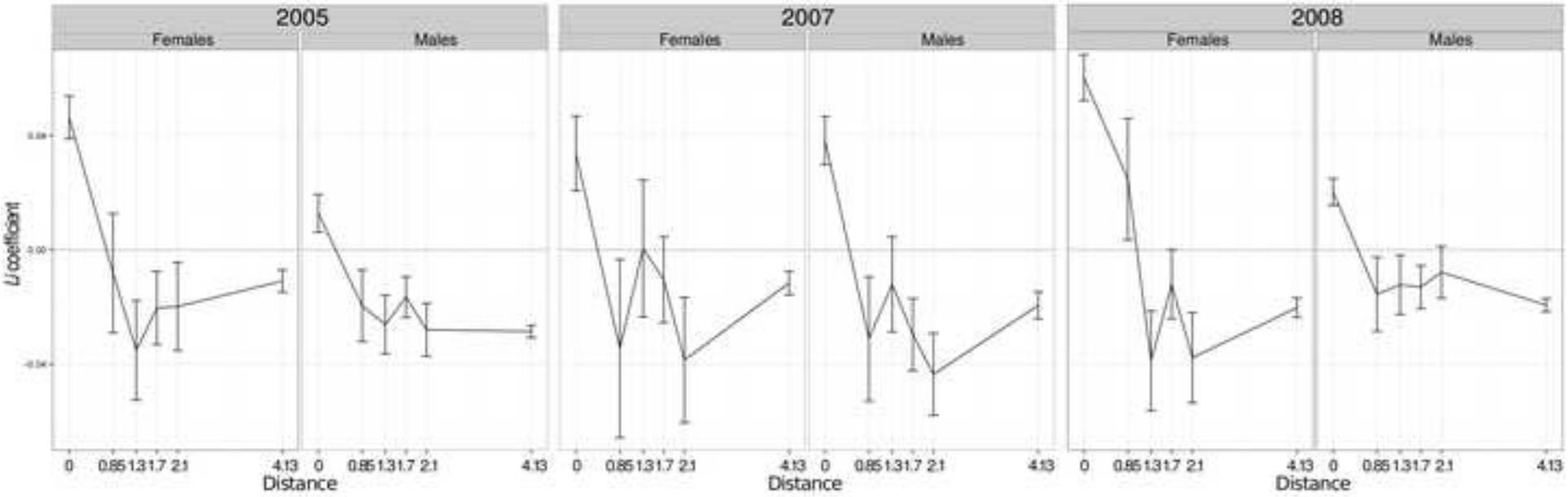

Figure6

Click here to download Figure Figure6_Dubois.tiff

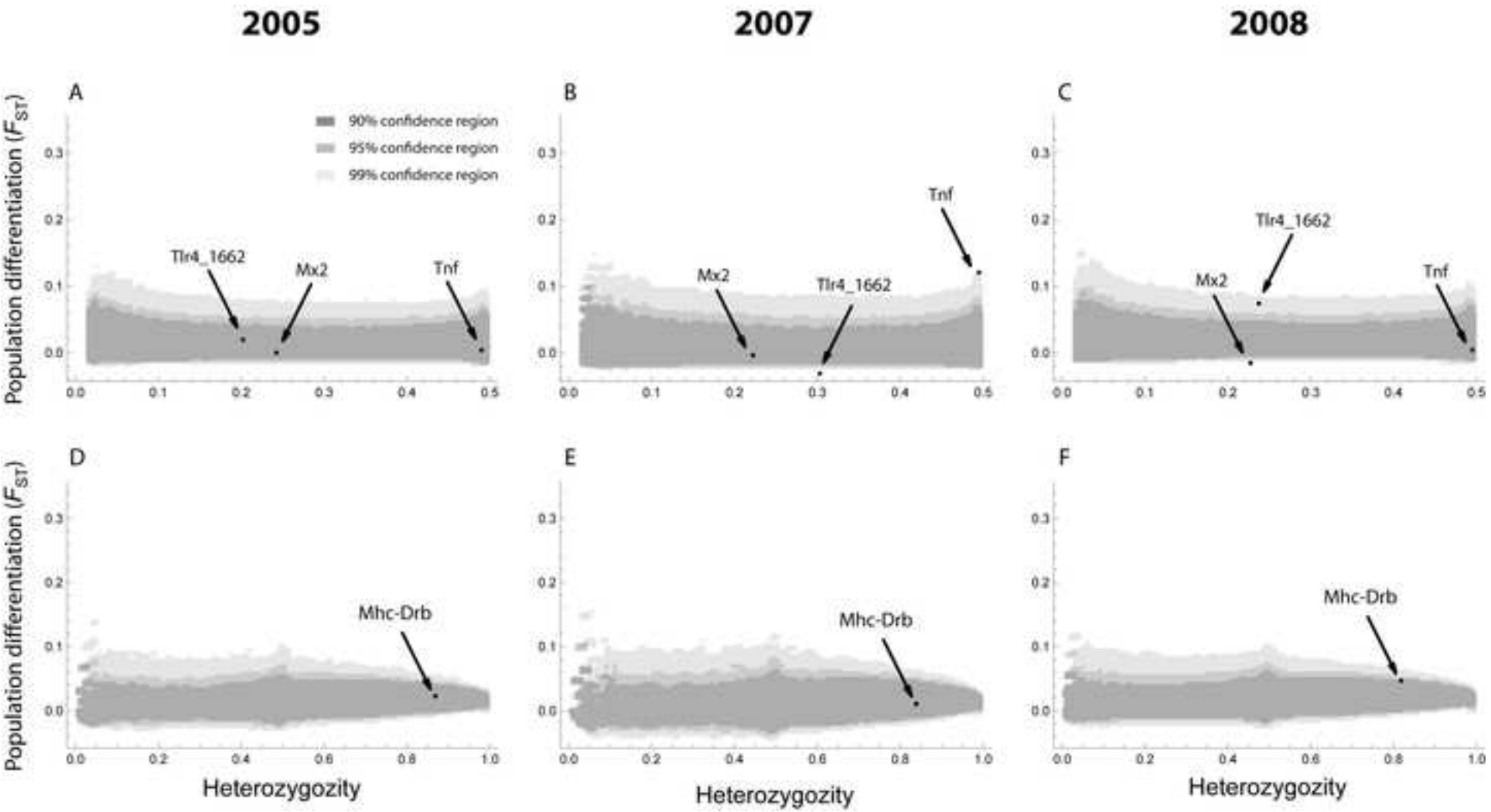

Figure7

Click here to download Figure Figure7_Dubois.tiff